

# Kinetics of Adsorption Competition of Pb-Cu and Pb-Methylene Blue in Aqueous Solution using Silica Gels from Coal Fly Ash

Yudi Aris Sulistiyono<sup>1,\*</sup>, Vivi Ruthmianingsih<sup>\*\*</sup>, Inayatul Mukarromah<sup>\*\*</sup>, Tanti Haryati<sup>\*\*</sup>, Novita Andarini<sup>\*\*</sup>, Suwardiyanto Suwardiyanto<sup>\*\*</sup>, Hamza Sani Rabiul<sup>\*\*\*</sup> and Gagus Ketut Sunnardianto<sup>\*\*\*\*</sup>

<sup>\*\*</sup>*Inorganic Material for Energy and Environmental Research Group, Department of Chemistry, Universitas Jember, Jl. Kalimantan 37, Jember, 68121, East Java, Indonesia.*

<sup>\*\*\*</sup>*Department of Applied Chemistry, Federal University Dutsin-ma, Katsina State, Nigeria.*

<sup>\*\*\*\*</sup>*Research Center for Quantum Physics, National Research and Innovation Agency (BRIN), Kawasan Puspitek Serpong, Tangerang Selatan, 15314, Banten, Indonesia.*

\*Corresponding Author: [yudi.fmipa@unej.ac.id](mailto:yudi.fmipa@unej.ac.id)

**Submitted** : 29-04-2021

**Revised** : 15-06-2021

**Accepted** : 05-08-2021

## ABSTRACT

Pollutants, such as Cu<sup>2+</sup> and Pb<sup>2+</sup>, are toxic and harmful to the ecosystem, and the removal of multicomponent pollutants from water systems can be challenging. Thus, the aim of this study investigated the adsorptive removal of Pb<sup>2+</sup> in the presence of Cu<sup>2+</sup> (Pb–Cu) and methylene blue (Pb–MB) ion competitors using coal fly ash-derived silica gels (SGs). The adsorptions were examined in a batch system under various experimental conditions (pH of the solution system and contact time). Additionally, the differences among the adsorption interactions of the functional groups on SG were determined via Fourier-transform infrared spectroscopy before and after the adsorption. The results revealed that the silanol group acted as the adsorption site. Moreover, in the single systems, the adsorption capacities of SG were ~84.03, 64.81, and 56.88 mg.L<sup>-1</sup> for MB, Cu<sup>2+</sup> and Pb<sup>2+</sup>, respectively. The kinetic adsorptions of the single and binary systems were best fitted to pseudo-second-order models. Compared with the single systems, the adsorption capacity and rate of each component in the binary solution systems decreased, indicating that the cationic competitors influenced the adsorption of Pb<sup>2+</sup>, or vice versa, depending on the amounts of charge and adsorption affinity.

**Keywords:** Binary pollutant; Adsorption competition; Silica gels; Adsorption kinetics

## INTRODUCTION

Water pollution caused by adverse industrial activities constitutes a serious threat. The concerns about access to pure water for human consumption and agricultural use, as well as the safety of aquatic life, have intensified the efforts towards water remediation (Bhat et al., 2015; Kushwaha et al., 2020). Numerous techniques and approaches, such as membrane separation, ion exchange, precipitation, flocculation and coagulation, bio- and photodegradation, and adsorption, have been employed to remove pollutants from water (Tamez et al., 2016; Liang et al., 2016). Among them, adsorption, which refers to the adherence of pollutants (atoms, ions, or molecules) onto the surface of an adsorbent, represents the key and foremost technology owing to its greenness, cost-effectiveness and efficiency; moreover, it comprises strategies for generating the required adsorbents (Karaca et al., 2018).

Pollutants, such as Pb, Cu, Cr and dye effluents, are largely produced via industrial activities (Kumar et al., 2019). A significant amount of these pollutants is noticeable and undesirable and their beyond-the-permissible-limit concentrations constitute serious threats to human and aquatic lives (Kavand et al., 2020). According to the United States Environmental Protection Agency regulation, the permissible concentrations of Pb<sup>2+</sup> and Cu<sup>2+</sup> pollutants in water systems are 0.015 and 1.3 mg.L<sup>-1</sup>, respectively (Chen et al., 2019). Additionally, even low concentrations of dyes ( $C < 1$  mg.L<sup>-1</sup>) can exert detrimental effects on aquatic ecosystems and

human health (Salleh et al., 2011). However, the presence of multicomponent pollutants further complicates their removal from water systems (Tamez et al., 2016).

To date, the adsorptive removal of these pollutants has been mostly facilitated with adsorbents that are derived from inexpensive materials, such as clay, zeolite, bio-sorbent, and agricultural and industrial wastes. Although agricultural wastes are potential adsorbents owing to their short process time and re-usability, industrial wastes, such as coal fly ash (CFA), are also good adsorbent candidates. Recently, the utilisation of CFA comprising SiO<sub>2</sub> (64.97 %), Al<sub>2</sub>O<sub>3</sub> (26.64 %) and Fe<sub>2</sub>O<sub>3</sub> (5.69 %) as the adsorption site attracted considerable attention (Adak et al., 2014). The adsorption activity of CFA owing to its composition has demonstrated sufficiency for the removal of pollutants (Gollakota et al., 2019). The adsorption capacities of CFA for heavy metals, such as Pb and Cu, can reach 5.1 and 4.4 mg.g<sup>-1</sup>, respectively (Alinnor, 2007). Moreover, its adsorption capacity for the removal of methylene blue (MB) can reach 7 mg.g<sup>-1</sup> (which is higher compared to those of heavy metals) (Wang et al., 2008). Additionally, the conversion of CFA into silica gels (SG) is among the strategies for increasing its adsorption capacity. In the previous studies, the adsorption capacity of MB using SG increased by 27.64% compared with that of CFA (Sulistiyo et al., 2017).

Here, we investigated the adsorptions of Pb(II) with heavy metal, Cu(II) (Pb–Cu), or cationic dye, MB (Pb–MB), competitors using CFA-derived SG as the adsorbent. Owing to the practicality viewpoint, the adsorption processes were studied in single and binary batch systems using an artificial solution. Among the oxides in CFA, SG was selected because it contains many silanol groups and exhibits well-defined surface properties, which facilitates the adsorption of cationic pollutants (Goscianska et al., 2013). This study also focused on the interaction between silica and the adsorbate, as well as the kinetics of the single and binary systems.

## **MATERIALS AND METHODS**

### **Coal Fly Ash sample and chemicals**

Coal fly ash was collected as a combustion waste from PT. POMI (Paiton, Probolinggo, East Java, Indonesia). H<sub>2</sub>SO<sub>4</sub> (95%, Sigma Aldrich), HCl (37%, Sigma Aldrich), NaOH (99%, Sigma Aldrich), Pb(NO<sub>3</sub>)<sub>2</sub> (99%, Sigma Aldrich), Cu(NO<sub>3</sub>)<sub>2</sub>·3H<sub>2</sub>O (99%, Sigma Aldrich) and MB (95%, Sigma Aldrich) were utilised as received from the manufacturers.

### **Preparation of SG**

SG was extracted and isolated from CFA, following the method that was described by Kalapathy et al., (2002). The fly ash was washed and oven dried before the synthesis. Next, NaOH (3 M) was added to the cleaned fly ash, then the mixture was refluxed at 90 °C for 2 h. Thereafter, the mixture was filtered to remove the solid residue. Next, HCl (1 M) was added to the filtrate and stirred until a pH value of 7 was obtained. Thereafter, the mixture was allowed to stand for 18 h. The resulting gel was collected, washed and oven dried overnight at 60 °C. Thereafter, the product was calcined at 550 °C for 4 h to remove its water and impurity contents.

## Characterisation of the SGs

SG was characterised via powder X-ray diffraction on a PANalytical X'pert diffractometer using Cu-K $\alpha$  radiation (40kV, 40 mA) at  $\lambda = 1,5404 \text{ \AA}$  with  $2\theta = 5^\circ\text{--}50^\circ$ . Further, its surface morphology was examined via scanning electron microscopy (SEM) employing an FEI Inspect-S50 microscope with 80.000 $\times$  magnification. The surface area and pore size were determined with a Quantachrome Instrument (NOVA 1200e). Furthermore, the functional groups on SG before and after the adsorption were characterised via Fourier-transform infrared (FTIR) using an FTIR Shimadzu Prestige 21 at a wavenumber of 400–4000  $\text{cm}^{-1}$ .

## Adsorption experiments (single and binary pollutants)

The adsorptions of the single and binary pollutants were performed at different pH values and times in a batch system using 0.1 g of the adsorbent and 25 mL of the adsorbates at room

temperature. The mixture was stirred at a constant agitation velocity (100 rpm) and different reaction times. The residual concentrations of the heavy metals were determined via atomic adsorption spectroscopy (Buck Scientific 205) and the dye concentrations were evaluated via ultraviolet–visible spectroscopy (Spectronic 20 Genesys, Thermo Fischer Scientific). Simultaneous adsorptions were also performed to investigate the Pb-adsorption mechanism on other existing pollutants, such as dyes (Pb–MB) or other heavy metals (Pb–Cu). The residual concentrations were measured as described in the single-pollutant experiment under similar conditions and the initial concentration of the binary mixed adsorbates (200  $\text{mg}\cdot\text{L}^{-1}$ ).

The amount of adsorbates on SG was calculated using Eq. (1):

$$q = \frac{(C_0 - C_e) \cdot V}{W} \quad (1)$$

where  $q$  is the adsorption capacity of the adsorbate per unit mass of adsorbent ( $\text{mg}\cdot\text{g}^{-1}$ ) at equilibrium;  $C_0$  and  $C_e$  are the initial and equilibrium concentrations ( $\text{mg}\cdot\text{L}^{-1}$ ) of the adsorbate, respectively;  $V$  is the volume of adsorbate solution (L) and  $W$  is the mass of the adsorbent (g).

Table 1. Linearity equations of the adsorption kinetic models

Kinetic Models	Formula
Pseudo-first-order by Lagergren	$\ln(q_e - q_t) = \ln q_e - k_1 t$
Pseudo-second-order by Ho and McKay	$\frac{t}{q_t} = \frac{1}{k_2 q_e} + \frac{t}{q_e}$
Intraparticle Diffusion	$q_t = k_t t^{1/2} + C$
Elovich Equation	$q_t = \frac{1}{\beta \ln(\alpha\beta)} + \frac{1}{\beta \ln t}$

## Kinetic studies of the adsorption process

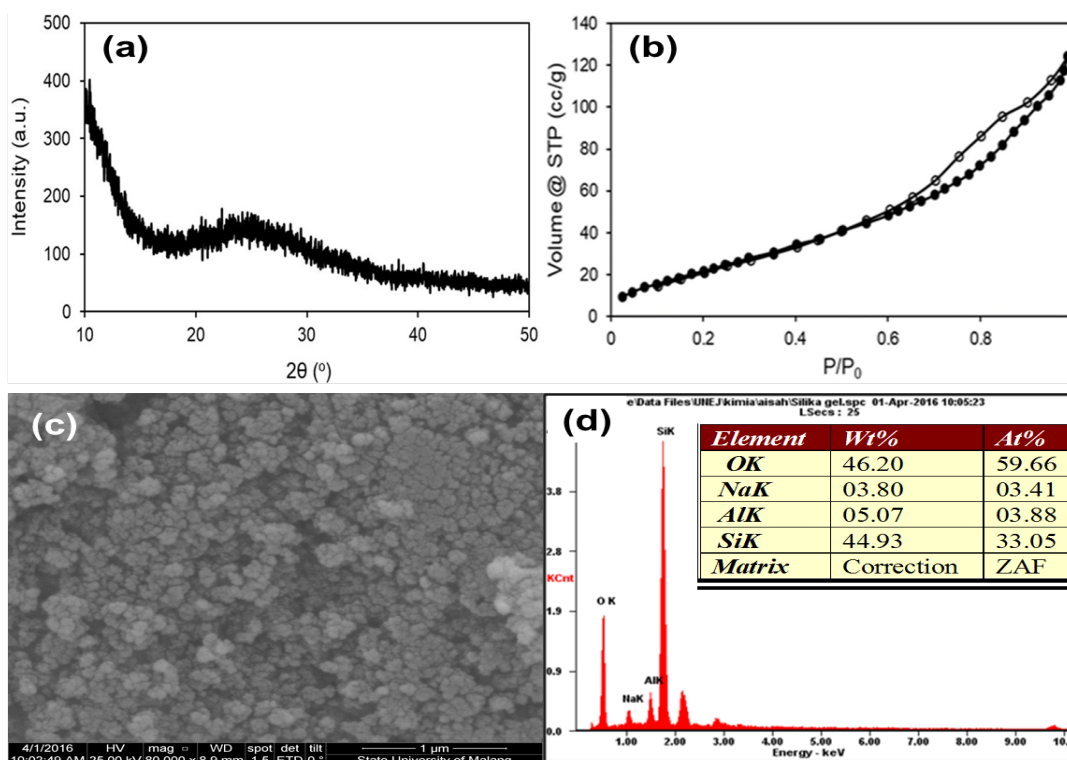
The kinetics of the adsorption was studied to evaluate the adsorption efficiency and determine the mechanism of the process (Ozdes et al., 2011). Some of the conventionally employed adsorption

kinetic models include the pseudo-first-order, pseudo-second-order, interparticle-diffusion and Elovich models (Table 1).

## RESULTS AND DISCUSSION

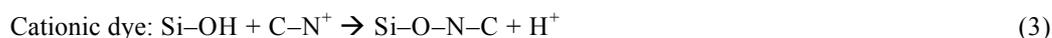
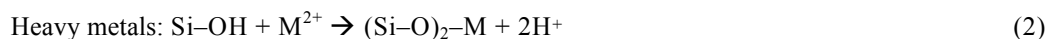
### Characterisation of Silica Gels

The X-ray diffractogram revealed that the amorphous structure of SG exhibited a broad peak at  $2\theta$  around  $25^\circ$  (Fig.1.a), and the SEM image revealed its irregular spherical shape (Fig.1.c). The removal of the metal impurities from the fly ash can be observed from its high Si and O percentages (Fig.1.d). The N<sub>2</sub> adsorption–desorption isotherm profile of the SG was classified as type IV (Fig.1.b), exhibiting a hysteresis loop from the capillary condensation in the pore with a surface area, pore size, and pore volume of 143.55 mg.g<sup>-1</sup>, 1.9 nm, and 0.279 cm<sup>3</sup>.g<sup>-1</sup>, respectively.



**Figure 1** Characterisation of the coal fly ash -derived SG via diffractogram X-ray (a), N<sub>2</sub> adsorption–desorption isotherm (b), scanning electron microscopy image (c), energy-dispersive X-ray analysis (d)

The FTIR analysis revealed the shifting functional groups on SG before and after the adsorption. The FTIR spectra (Fig. 2) revealed that the stretching and bending of the hydroxyl group (–OH) from the silanol group (Si–OH) at peaks of 1635.69 and 3448.84 cm<sup>-1</sup>, respectively, while the peaks at 461.00, 715.61, and 1057.03 cm<sup>-1</sup> corresponded to the bending, stretching symmetry, and stretching asymmetry of the siloxane group (Si–O–Si), respectively. As illustrated by the reduced peak area at 1635.69 and 3448.84 cm<sup>-1</sup>, Figs.2 b–f reveal that the adsorption process affected the Si–OH group, which was the active site of silica. Further, the cationic exchange of Si–OH on the silica surface was the most relevant but not the sole mechanism that caused these decreasing peaks (Kutzner et al., 2014). As exhibited in Schemes 2 and 3, Hernández-Montoya and co-worker also reported that the cation exchange was the most relevant interaction model for the adsorption using Si–OH on the surface of the materials (Hernández-Montoya et al., 2013).



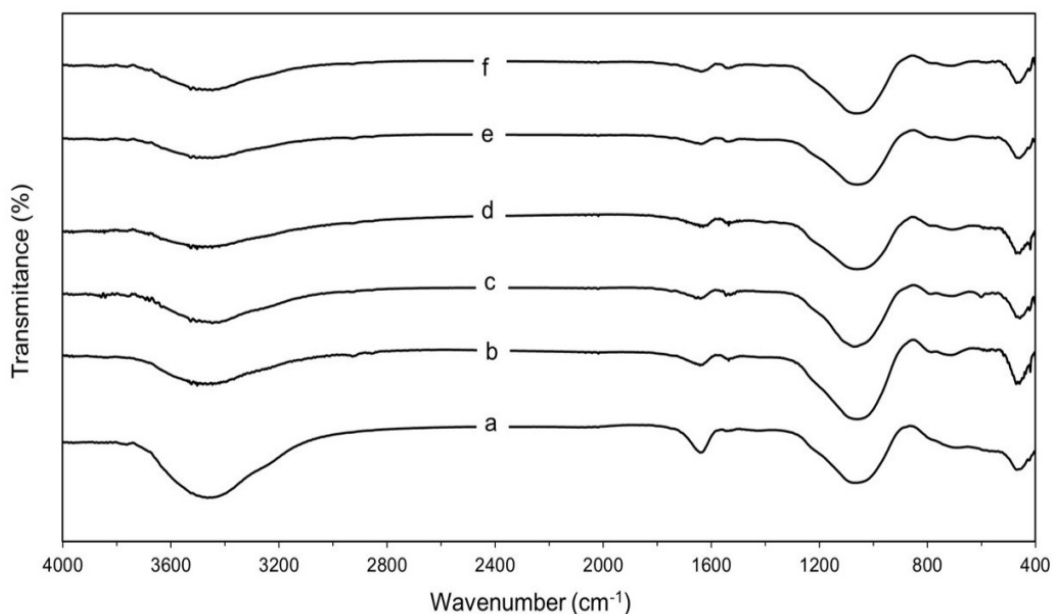


**Figure 2** Fourier-transform infrared Spectra of SiO<sub>2</sub> (a), SiO<sub>2</sub>/Pb (b), SiO<sub>2</sub>/Cu (c), SiO<sub>2</sub>/MB (d), SiO<sub>2</sub>/Pb–MB (e) and SiO<sub>2</sub>/Pb–Cu (f)

### Effect of pH on the adsorption capacity

The different adsorption behaviours of Pb, Cu and MB, which were observed at different pH values (1–10, Fig. 3), indicate the dissociation processes of the functional groups and surface charges of SG. The pH affects the surface charge of the adsorbent, the degree of the ionisation of the adsorbate and the degree of the dissociation of the functional groups on the active sites of the adsorbent (Silva et al., 2012). The surface charge of SG changed from protonated (Si–OH) to deprotonated (Si–O<sup>–</sup>) across different pH solutions.

The SG adsorbent contained species of Si–OH on its surface, where the pH of their interactions with Si–OH and Si–O<sup>–</sup> were < 6, while that with only Si–O<sup>–</sup> was > 6 (Adam et al. (2013); Wu et al., 2013). The adsorption process of Si–OH proceed via a combined mechanism involving the electrostatic interactions with the cationic adsorbate and cationic exchange, the surface-complexation phenomena and the van der Waals effects (Valdés et al., 2012). The negative charges on the surface of silica exhibited an electrochemical interaction with the cationic molecules of the adsorbate (Huang et al., 2011). Moreover, the pH also affects the metal species in the solution (Niu et al., 2013).

The adsorption capacity of Pb in a single solution using SG increased as the pH value increased from 2 to 6, where the gradual increase in the negative charges at the surface of SG promoted the Pb<sup>2+</sup> interaction therein. However, the adsorption capacity decreased with the increasing pH value (pH > 6) owing to the decreasing electrostatic interaction between Si–O<sup>–</sup> and Pb<sup>2+</sup>, which is due to the increasing concentrations of Pb(OH)<sup>+</sup> and Pb(OH)<sub>2</sub>. However, Pb(OH)<sup>+</sup> can interact with the Si–O<sup>–</sup> species through hydrogen bonding (Papandreou et al., 2011). In this study, the highest amount of Pb that was adsorbed on SG was 56.878 mg.L<sup>–1</sup> at the optimum pH (6), and this result corresponds to the finding of Al-Zboon et al. (2011).

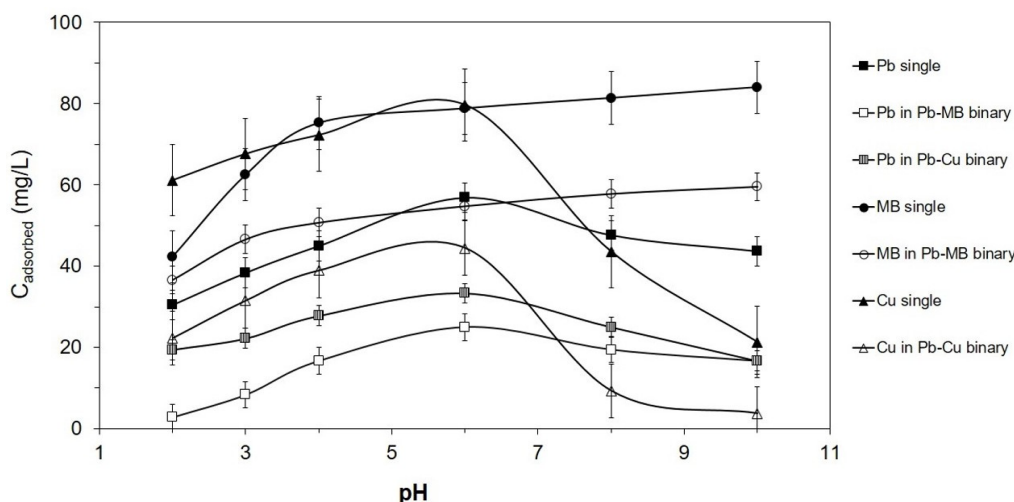


**Figure 3** Models of the adsorptions of  $Pb^{2+}$  by silica gels from various pH systems containing  $Pb^{2+}$  and other competitors, namely methylene blue and  $Cu^{2+}$ , as single and binary systems

The effect of the pH was also investigated in the adsorptions of MB and Cu as competitors in the single system. A similar pattern to that of Pb adsorption was observed for  $Cu^{2+}$  but with a higher adsorption capacity (79.63  $mg.L^{-1}$ ). Compared with Pb, MB achieved an optimum adsorption capacity at pH 10 (84.03  $mg.L^{-1}$ ). However, the MB species existed as  $H_2MB^+$  and  $MB^+$  under acidic and basic conditions, respectively. The high concentration of the positive charge from  $MB^+$  increased its interaction with  $Si-O^-$ .

In the binary systems, the adsorption capacity of  $Pb^{2+}$  decreased by 56.05% and 41.40% in the presence of MB and  $Cu^{2+}$ , respectively. Similarly, MB and  $Cu^{2+}$  were also reduced by 29.12% and 44.19%, respectively. The competitive interaction proceeded on the surface of SG, and the adsorbates that were obtained via the multicomponent adsorption were in the following order:  $MB > Cu^{2+} > Pb^{2+}$  (Ding et al., 2016). Although we anticipated that MB with a bulky structure would exhibit a low adsorption affinity, a contrary result was observed. The ionisation state also contributed to the chemisorption-type adsorption; in this regard, the particle size did not play a significant role (Noroozi and Sorial, 2013). Based on the ionisation state, MB (+1) experienced less competition compared with Pb (+2) or Cu (+2) in interacting with surface  $Si-O^-$ . Regarding

Pb and Cu with similar ionisation states (+2), Cu with the stronger reducing capacity exhibited a higher affinity to  $Si-O^-$  and could displace the Pb interaction on the surface (Zhan et al., 2018).

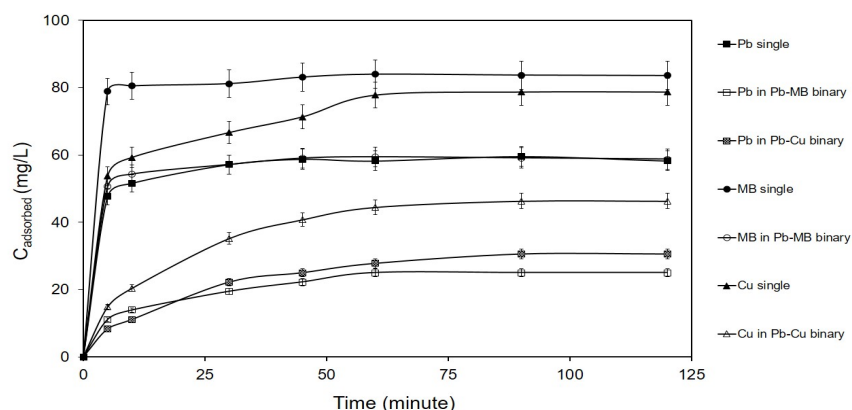


**Figure 4** Time variation of the adsorption of  $Pb^{2+}$  with the competitors, methylene blue and  $Cu^{2+}$ , by silica gels in the single and binary systems

## **Effect of the contact time on the adsorption process**

The effect of the contact time on the adsorption process was investigated in a time range of 5–120 min at the optimum pH value for the single and binary adsorption systems. The results indicated that the adsorption capacity increased with the increasing contact time and that the optimum adsorption was obtained within 60 min. Beyond this optimum time, the adsorption capacity remained unchanged (Fig.4). In the single adsorption system, the rapid removal of the adsorbate occurred within 30 min, beyond which it further increased slightly up to 60 min where it achieved an adsorption equilibrium. These conditions revealed that the adsorption process followed a two-step mechanism, namely, the rapid adsorption involving external–internal diffusion and the slow uptake controlled by intraparticle diffusion until it reached equilibrium (Michard et al., 1996). Ozdes and co-workers observed that the rapid adsorption occurred when the metal ions interacted with the adsorbent, exposing additional active sites at the onset of the adsorption (Ozdes et al., 2011). Huang et al. (2011) reported the same phenomenon. The uptake was dramatically rapid within the first 10 min, after which the adsorption rate decreased up to the optimum time (60 min) during which the highest removal was observed.

## **Kinetics of the adsorptions**

The adsorption kinetics of the single and binary systems onto SG were examined via several kinetic models, such as the pseudo-first-order, pseudo-second-order, interparticle-diffusion and Elovich models to determine the adsorption efficiency. The adsorption models followed the pseudo-second-order kinetics, with a correlation coefficient ( $R^2$  values) of  $\sim 1$  (Table 2), indicating that the adsorbent and adsorbate affected the adsorption process. The model is consistent with the calculated ( $q_e$  calc.) and experimental ( $q_e$  exp.) amounts of the adsorbed adsorbents.

Based on the model, the adsorption rate of  $\text{Cu}^{2+}$  was the highest, followed by MB and  $\text{Pb}^{2+}$  in the single system. This is because  $\text{Cu}^{2+}$  exhibited the smallest atomic size, correlating with the possibility of a rapid dispersion on the silica surface. Although MB exhibited a higher molecular weight than  $\text{Pb}^{2+}$ , its adsorption rate was higher; this is because of its +1 molecular charge, which facilitates its easy electrostatic interaction with the charge on the silica surface. Hernández-Montoya et al. (2013) also reported that the hydroxyl groups exhibit a higher affinity for the cationic dye than for the heavy metal. The adsorption rate of the binary system was lower than that of the single one. Furthermore, MB and  $\text{Pb}^{2+}$  occupied different active sites on the silica surface with less competition. However, in the Pb and Cu binary systems, the competition was stronger than in the single system because of the decreased adsorption rate. The adsorption rates of the binary  $\text{Pb}^{2+}$  and  $\text{Cu}^{2+}$  systems decreased by  $\sim 10$  and 20 folds, respectively.

**Table 1** Adsorption kinetics Pb<sup>2+</sup> with the competitors, methylene blue and Cu<sup>2+</sup>, on silica gels in the single and binary systems

Adsorbate		Pb			MB		Cu	
		Single	Binary in MB	Binary in Cu	Single	Binary	Single	Binary
<b>q<sub>e</sub> Exp. (mg/g)</b>		14.88	4.17	7.64	20.97	14.85	19.68	11.55
Pseudo-first-order model	k <sub>1</sub> (min <sup>-1</sup> )	1.5 × 10 <sup>-3</sup>	8.4 × 10 <sup>-3</sup>	1.0 × 10 <sup>-2</sup>	5 × 10 <sup>-4</sup>	1 × 10 <sup>-3</sup>	3.2 × 10 <sup>-3</sup>	8.8 × 10 <sup>-3</sup>
	q <sub>e</sub> (mg.g <sup>-1</sup> )	1.15	2.17	2.58	1.05	1.10	1.35	2.21
	R <sup>2</sup>	0.536	0.701	0.688	0.678	0.536	0.774	0.659
Pseudo-second-order model	k <sub>2</sub> (g.mg <sup>-1</sup> .min <sup>-1</sup> )	6.8 × 10 <sup>-2</sup>	1.5 × 10 <sup>-2</sup>	5.9 × 10 <sup>-3</sup>	9.8 × 10 <sup>-2</sup>	9.4 × 10 <sup>-2</sup>	1.1 × 10 <sup>-1</sup>	5.6 × 10 <sup>-3</sup>
	q <sub>e</sub> (mg.g <sup>-1</sup> )	14.82	4.73	8.99	21.09	14.84	20.41	13.11
	R <sup>2</sup>	0.999	0.990	0.997	0.999	0.999	0.998	0.998
Interparticle-diffusion model	k <sub>t</sub> (mg.g <sup>-1</sup> .min <sup>-1/2</sup> )	3.0 × 10 <sup>-1</sup>	3.4 × 10 <sup>-1</sup>	6.8 × 10 <sup>-1</sup>	1.4 × 10 <sup>-1</sup>	2.2 × 10 <sup>-1</sup>	7.6 × 10 <sup>-1</sup>	9.5 × 10 <sup>-1</sup>
	C	12.00	0.98	1.09	19.60	12.77	12.42	2.63
	R <sup>2</sup>	0.728	0.899	0.917	0.823	0.726	0.920	0.886
Elovich Equation	α (mg g <sup>-1</sup> .min <sup>-1</sup> )	1.3 × 10 <sup>5</sup>	8.2 × 10 <sup>-1</sup>	10.3 × 10 <sup>-1</sup>	1.3 × 10 <sup>20</sup>	3.3 × 10 <sup>7</sup>	229.32	21.1 × 10 <sup>-1</sup>
	β (g.mg <sup>-1</sup> )	1.10	1.06	0.52	2.47	1.49	0.47	0.37
	R <sup>2</sup>	0.891	0.956	0.983	0.975	0.888	0.969	0.975

## CONCLUSIONS

In summary, SG with an amorphous structure and irregular spherical shapes was successfully synthesised from CFA. As a material adsorbent, the Si–OH group of SG interacted with Pb<sup>2+</sup> and its competitors (MB and Cu<sup>2+</sup>), exhibiting decreasing peaks in wavenumbers of 1635.69 and 3448.84 cm<sup>-1</sup>. The maximum uptakes of Pb<sup>2+</sup> and Cu<sup>2+</sup> were obtained at pH 6 while that of MB was obtained at pH 10, and the optimum contact time was 60 min at room temperature. In the single systems, the amount of adsorbates followed the order, MB > Cu<sup>2+</sup> > Pb<sup>2+</sup>. In the binary solution systems, the adsorption capacities of Pb<sup>2+</sup> decreased in the presence of MB and Cu<sup>2+</sup>, while that of each competitor decreased compared with their single system.

Furthermore, following the pseudo-second-order kinetic models, the adsorption rate of each adsorbate decreased in the Pb–MB and Pb–Cu binary systems. Our findings clarify the adsorption capacity and rate of each adsorbate in single and binary systems, which are influenced by the number of charges, as well as the strength of the adsorption affinity with SG.

## REFERENCES

- Adak D., Sarkar M., & Mandal S.** 2014. Effect of nano-silica on strength and durability of fly ash based geopolymer mortar. *Constr. Build. Mater.* 70, 453–459.
- Adam F., Appaturi J.N., Khanam Z., Thankappan R., & Nawi M.A.M.** 2013. Utilization of tin and titanium incorporated rice husk silica nanocomposite as photocatalyst and adsorbent for the removal of methylene blue in aqueous medium. *Appl. Surf. Sci.* 264: 718–726.
- Alinnor I.J.** 2007. Adsorption of heavy metal ions from aqueous solution by fly ash. *Fuel.* 86:853–857.
- Al-Zboon K., Al-Harashsheh M.S., & Hani F.B.** 2011. Fly ash-based geopolymer for Pb removal from aqueous solution. *J. Haz. Mater.* 188: 414–421.
- Bhat A., Megeri G.B., Thomas C., Bhargava H., Jeevitha C., Chandrashekar S., & Madhu G.M.** 2015. Adsorption and optimization studies of lead from aqueous solution using  $\gamma$ -Alumina. *J. Env. Chem. Eng.* 3: 30–39.
- Chen C., Chen Q., Kang J., Shen J., Wang B., Guo F., & Chen Z.** 2019. Hydrophilic triazine-based dendron for copper and lead adsorption in aqueous systems: Performance and mechanism. *J. of Mol. Liquids.* 298: 112031.
- Ding G., Wang B., Chen L., & Zhao S.** 2016. Simultaneous adsorption of methyl red and methylene blue onto biochar and an equilibrium modeling at high concentration. *Chemosphere.* 163: 283–289.
- Gollakota A.R.K., Volli V., & Shu C.M.** 2019. Progressive utilisation prospects of coal fly ash: A review. *Sci. Total Env.* 672: 951–989.
- Goscianska J., Olejnik A., & Pietrzak R.** 2013. Adsorption of L-phenylalanine onto mesoporous silica. *Mater. Chem. and Phys.* 142: 586-593.
- Hashemian S., Sadeghi B., & Mangeli M.** 2015. Hydrothermal synthesis of nano cavities of Al-MCF for adsorption of indigo carmine from aqueous solution. *J. Ind. Eng. Chem.* 21: 423–427.
- Hernández-Montoya V., Pérez-Cruz M.A., Mendoza-Castillo D.I., Moreno-Virgen M.R., & Bonilla-Petriciolet A.** 2013. Competitive adsorption of dyes and heavy metals on zeolitic structures. *J. Env. Manag.* 116: 213–221.
- Huang C.H., Chang K.P., Ou H.D., Chiang Y.C., & Wang C.F.** 2011. Adsorption of cationic dyes onto mesoporous silica. *Microporous and Mesoporous Materials.* 141: 102–109.

- Kalapathy U., Proctor A., & Shultz J.** 2002. An improved method for production of silica from rice hull ash. *Bioresource Technology*. 85: 285–289.
- Karaca H., Altıntığ E., Türker D., & Teker M.** 2018. An evaluation of coal fly ash as an adsorbent for the removal of methylene blue from aqueous solutions: kinetic and thermodynamic studies. *J. Dis. Sci. Tech.* 39: 1800–1807.
- Kavand M., Eslami P., & Razeh L.** 2020. The adsorption of cadmium and lead ions from the synthesis wastewater with the activated carbon: Optimization of the single and binary systems. *J. Water Proc. Eng.* 34: 101151.
- Kumar G.V.S.R.P., Malla K.A., Yerra B., & Rao K.S.** 2019. Removal of Cu(II) using three low-cost adsorbents and prediction of adsorption using artificial neural networks. *Applied Water Sci.* 9: 1–9.
- Kushwaha A., Rani R., & Patra J.K.** 2020. Adsorption kinetics and molecular interactions of lead [Pb(II)] with natural clay and humic acid. *Int. J. Env. Sci. Tech.* 17: 1325–1336.
- Kutzner S., Schaffer M., Bornick H., Licha T., & Worch E.** 2014. Sorption of the organic cation metoprolol on silica gel from its aqueous solution considering the competition of inorganic cations. *Water Research*. 54: 273–283.
- Liang S., Ye N., Hu Y., Shi Y., Zhang W., Yu W., Wu X., & Yang J.** 2016. Lead adsorption from aqueous solutions by a granular adsorbent prepared from phoenix tree leaves. *RSC Advance*. 6: 25393–25400.
- Michard P., Guibal E., Vincent T., & Le Cloirec P.** 1996. Sorption and desorption of uranyl ions by silica gel: pH, particle size and porosity effects. *Microporous Materials*. 5: 309–324.
- Niu Y., Qu R., Sun C., Wang C., Chen H., Ji C., Zhang Y., Shao X., & Bu F.** 2013. Adsorption of Pb(II) from aqueous solution by silica-gel supported hyperbranched polyamidoamine dendrimers. *J. Haz. Mater.* 244–245: 276–286.
- Noroozi B., & Sorial G.A.** 2013. Applicable models for multi-component adsorption of dyes: A review. *J. Env. Sci.* 25: 419–429.
- Ozdes D., Duran C., & Senturk H.B.** 2011. Adsorptive removal of Cd(II) and Pb(II) ions from aqueous solutions by using Turkish illitic clay. *J. Env. Manag.* 92, 3082–3090.
- Papandreou A.D., Stournaras C.J., Panias D., & Paspaliaris I.** 2011. Adsorption of Pb(II), Zn(II) and Cr(III) on coal fly ash porous pellets. *Minerals Engineering*. 24, 1495–1501.
- Salleh M.A.M., Mahmoud D.K., Karim W.A.W.A.K., & Idris A.** 2011. Cationic and anionic dye adsorption by agricultural solid wastes: a comprehensive review. *Desalination*. 280: 1–13.
- Sulistiyo Y.A., Andriana N., Piluharto B., & Zulfikar Z.** 2017. Silica Gels from Coal Fly Ash as Methylene Blue Adsorbent: Isotherm and Kinetic Studies. *Bull. Chem. React. Eng. & Catal.* 12: 263.
- Tamez C., Hernandez R., & Parsons J.G.** 2016. Removal of Cu (II) and Pb (II) from aqueous solution using engineered iron oxide nanoparticles. *Microchemical Journal*. 125: 97–104.
- Valdés H., Tardón R.F., & Zaror C.A.** 2012. Role of surface hydroxyl groups of acid-treated natural zeolite on the heterogeneous catalytic ozonation of methylene blue contaminated waters. *Chemical Engineering Journal*. 211–212: 388–395.
- Wang S., Ma Q., & Zhu Z.H.** 2008. Characteristics of coal fly ash and adsorption application. *Fuel*. 87: 3469–3473.
- Wu Y., Cao J., Yilihan P., Jin Y., Wen Y., & Zhou J.** 2013. Adsorption of anionic and cationic dyes from single and binary systems by industrial waste lead–zinc mine tailings. *RSC Advance*. 3: 10745.
- Yao Z.T., Ji X.S., Sarker P.K., Tang J.H., Ge L.Q., Xia M.S., & Xi Y.Q.** 2015. A comprehensive review on the applications of coal fly ash. *Earth-Science Reviews*. 141: 105–121.

**Zhan W., Xu C., Qian G., Huang G., Tang X., & Lin B.** 2018. Adsorption of Cu(II), Zn(II), and Pb(II) from aqueous single and binary metal solutions by regenerated cellulose and sodium alginate chemically modified with polyethyleneimine. *RSC Advance*. 8: 18723–18733.